Chapter 2. Basic Atomic Physics

Academic and Research Staff

Professor Daniel Kleppner, Professor David E. Pritchard, Dr. Min Xiao

Visiting Scientists and Research Affiliates

Dr. Theodore W. Ducas[1]

Graduate Students

Kevin R. Boyce, Pin P. Chang, Eric A. Cornell, Michael W. Courtney, Chris R. Ekstrom, Thomas R. Gentile, Kristian Helmerson, Long Hsu, Barbara J. Hughey, Chun-Ho Iu, Michael A. Joffe, David W. Keith, Robert P. Lutwak, Bruce G. Oldaker, Scott Paine, Ke-Xun Sun, George R. Welch

Undergraduate Students

Deborah Kuchnir, James P. Schwonek, Quentin Turchette

Technical and Support Staff

Carol A. Costa

2.1 Experimental Study of Small Ensembles of Atoms in a Microwave Cavity

Sponsor

Joint Services Electronics Program
Contract DAAL03-89-C-0001

Project Staff

Barbara J. Hughey, Thomas R. Gentile, Dr. Theodore W. Ducas, Professor Daniel Kleppner

Cavity quantum electrodynamics — the study of interactions of individual atoms with quantum fields in cavities — has grown into an active area of quantum optics.[2] A seminal experiment in this area was the inhibition of spontaneous emission of an excited atom, first demonstrated in our laboratory some years ago.[3] During this past year, we have completed a study of the evolution of small ensembles of atoms in a microwave cavity. Our goal is to observe the dynamics of an atom-vacuum system in the quantum regime.

The states of our collective N-atom system are Dicke states.[4] The total atom-field Hamiltonian for the system is[5]

$$H_{tot} = H_A + H_F + H_{AF}$$

$$= \hbar\omega_0 D^\circ + \hbar\omega(a^\dagger a + \tfrac{1}{2})$$

$$+ \tfrac{1}{2}\hbar\omega_a(aD^+ + a^\dagger D^-), \qquad (1)$$

---

[1] Department of Physics, Wellesley College, Wellesley, Massachusetts.

[2] S. Haroche and D. Kleppner, *Phys. Today B* 42(1): 24 (1989).

[3] R.G. Hulet, E.S. Hilfer, and D. Kleppner, *Phys. Rev. Lett.* 55: 2137 (1985).

[4] R.H. Dicke, *Phys. Rev. B* 93: 99 (1954).

[5] S. Haroche, in *New Trends in Atomic Physics,* eds. G. Grynberg and R. Stora (Amsterdam: North Holland, 1984), 190.

where H_A and H_F are the atomic and field Hamiltonians, respectively, and H_{AF} describes the atom-field interaction. a and $a^\dagger$ are the conventional destruction and creation operators for the electromagnetic field. D^+ and D^- are collective atomic raising and lowering operators, respectively, that act on the Dicke states like standard angular momentum raising and lowering operators. D° acts on the Dicke states like the z – component of the angular momentum operator.

The evolution of the system can be described by the density matrix equation

$$\frac{d\rho_{A+F}}{dt} = \frac{1}{i\hbar}[H_{tot}, \rho_{A+F}] + \Lambda_F \rho_{A+F}, \quad (2)$$

The last term in equation (2) accounts for dissipation. The probability that a member of the system is excited at time t is related to the expectation value of D° by

$$P_e(t,N) = \frac{1}{N} < D^\circ > + \frac{1}{2} \quad (3)$$

For more than fifty atoms, an alternative method based on the Bloch vector model becomes more practical than the above approach. The time derivatives of the quantum mechanical operators D°, D^+, and $a^\dagger$ are found in the Heisenberg picture. The atomic operators are related to the components (η, ρ) of the Bloch vector, a classical angular momentum vector with length $J = N/2$
$D^\circ \rightarrow \eta \equiv \frac{1}{2}N \cos\theta$ and $D^+ \rightarrow \rho \equiv \frac{1}{2}N \sin\theta e^{i\phi}$, where θ and ϕ are the standard angles in spherical coordinates. The field operator $a^\dagger$ is identified with ε, a classical electric field in the cavity. The evolution of the system is described by[6]

$$\frac{d\eta}{dt} = \frac{-i\omega_a}{2}(\varepsilon^*\rho - \varepsilon\rho^*), \quad (4a)$$

$$\frac{d\rho}{dt} = -i\omega_a \varepsilon \eta, \quad (4b)$$

$$\frac{d\varepsilon}{dt} = i\delta\varepsilon - \gamma\varepsilon + \frac{i\omega_a}{2}\rho + \tilde{F}^\dagger(t) \quad (4c)$$

where $\delta \equiv \omega - \omega_o$ Equation (4c) includes a damping term and a random force $\tilde{F}^\dagger(t)$ that account for the coupling of the radiation mode to the thermal reservoir of the cavity walls. It can be shown that the probability of excitation at time t is given by

$$P_e(t,N) = \frac{1}{N} < \eta(t,N,\theta(0)) >_{\theta(0)} + \frac{1}{2} \quad (5)$$

where the average over $\theta(0)$ is carried out over an appropriate distribution of initial angles arising from thermal fluctuations.

There is no general way to parametrize the behavior of the atom-cavity system, but for underdamped motion one feature is particularly easy to observe experimentally: this is the time τ_{min} at which $P_e(t,N)$ achieves its first minimum. We define the "collapse frequency" ν_{col} by

$$\nu_{col} \equiv (2\tau_{min})^{-1} \quad (6)$$

Although $P_e(t,N)$ is a complicated function of the system parameters, Haroche[5] has pointed out that the variation of ν_{col} with the number of atoms N can be accurately parameterized by

$$\nu_{col}(N) = \frac{a\sqrt{N}}{b + \ln N} \quad (7)$$

where a and b are adjustable parameters that depend on ω_a, γ, and β. The accuracy of this expression is illustrated by figure 1 which displays values of ν_{col} obtained from the exact solution [equation (3)] for $N \leq 50$ and from the Bloch method [equation (5)] for $N \geq 200$, along with the best fit of equation (7) to the calculations.

The experiments employ an atomic beam of calcium Rydberg atoms and a split superconducting cavity operated at 35 GHz. At the ambient temperature of 2 K, the mean blackbody photon number is 0.8. Selective

[6] B.J. Hughey, *Cavity Modified Atom-Photon Interaction,* Ph.D. diss., Dept. of Physics, MIT, 1989.

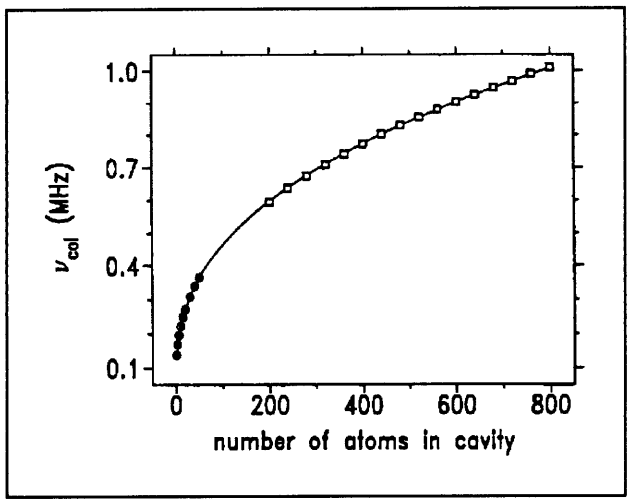

Figure 1. Dependence of the "collapse" frequency ν_{col} on number of atoms N for $Q = 1.2 \times 10^7$ and T = 2.17K. The filled circles are obtained from the exact method and the open squares from the Bloch method, as discussed in the text. The solid curve is a fit of the calculations to equation (7), which yields a = 0.3187MHz and b = 2.245.

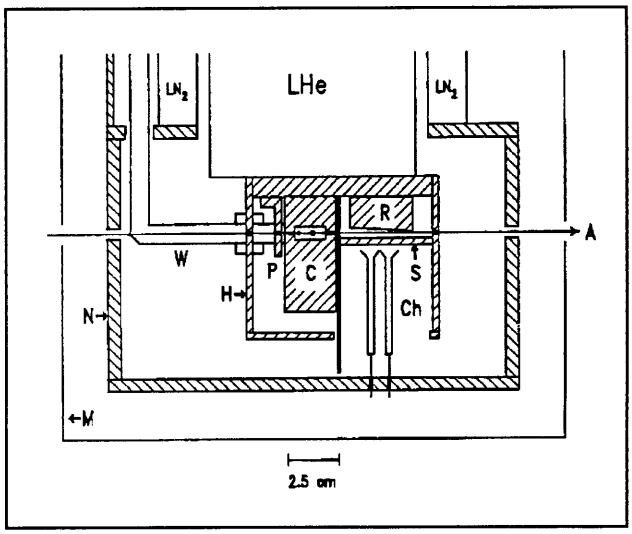

Figure 2. Diagram of the apparatus, side view. A: atomic beam, H: liquid helium temperature shield, N: liquid nitrogen temperature shield, M: single layer mu-metal shield, P: collimating plate of 2 channel field ionization detector, C: cavity, R: ramped plate, S: slotted plate, Ch: channel electron multipliers, W: waveguide, L: laser beams, B: waveguide holder, Co: coupler. The tuning mechanism is not shown for clarity.

field ionization allows us to monitor simultaneously the populations of the initial and final states. The time evolution of the atomic system is probed by "Stark switching." The collective oscillations of energy between ensembles of atoms and a cavity with $Q > 10^7$ are being studied for one to several hundred atoms.

The experiment is carried out with the apparatus shown in figure 2. A calcium atomic beam is prepared in the 46p state (abbreviation for the 4s46p $^1P_1$ state) inside the cavity using a three-step pulsed dye laser system. The final laser beam is polarized along the cavity electric field so that the 46p(m=0) state is excited relative to this quantization axis. The two states involved in the atom-cavity oscillations are thus the 46p(m=0) (upper state) and 46s (lower state). The frequency of the 46p → 46s transition in calcium is 35.332 GHz; the atom-cavity coupling frequency $\omega_a/2\pi$ calculated for this transition and our cavity dimensions is 105 kHz. Observing underdamped behavior for a single atom in the cavity requires $Q > 2 \times 10^5$. To avoid undesirable effects of blackbody radiation, the one-atom experiments require temperatures $\lesssim$2K, for which $\bar{n} \lesssim 0.8$.

The atoms are excited inside the cavity. The mean transit time to the cavity exit is 18 μsec, which corresponds to two cycles of the single-atom-cavity oscillation. After the atoms exit the cavity, they enter the detector region where selective field ionization is used to detect and differentiate the two states. We measure $\bar{P}_e(t, \bar{N})$ for each value of $\bar{N}$ by scanning the time t when a 200 mV pulse is applied between the cavity halves. ($\bar{N}$ is the mean number of atoms in the cavity.) In this way, we count the number of atoms detected in the 46p and 46s states as a function of the atom-cavity interaction time. Sample data are shown in figure 3.

An important feature of the experiment is the use of a split superconducting cavity. By applying an electric field between the two halves, the atomic resonance can be shifted far from resonance with the cavity, thereby terminating the atom-cavity interaction. This effectively freezes the atomic population at the moment at which the voltage pulse is applied. By using a carefully designed choke groove structure, we suppress leakage from the cavity and achieve a quality factor $Q > 10^7$ in niobium and lead-plated copper cavities.

A series of time evolution curves for various values of $\bar{N}$ was studied. Figures 4 and 5

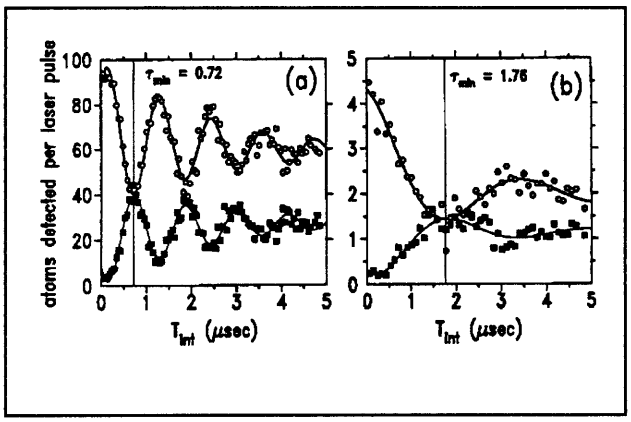

Figure 3. Observed atom-cavity oscillations for $Q = 1.18 \times 10^7$ and $T = 2.17K$ for two values of $\bar{N}_d$. The solid curves are fits of the data to damped sinusoids, from which ν_{col} is extracted. The open circles are the atoms detected in the 46p state, and the filled squares are the atoms detected in the 46s state. T_{int} is the atom-cavity interaction time.

display some of the data along with the calculated time evolution curves.

We also compared our results with theory for a single atom in the cavity. Single atom experiments are of special significance because they represent the limit of small systems. Furthermore, they have the experimental advantage of being free of much of the uncertainty in detection efficiency, assuming that the mean number of atoms detected per pulse is small compared to unity. For these studies, we generally operated with an average of 0.04 atoms detected per laser pulse. The observed and calculated evolution of a single atom in the cavity with $Q = 1.5 \times 10^6$ and $T = 1.95K$ are shown in figure 6. We believe that the damping which is evident in the data is due to stray electric and magnetic fields, and possibly thermal effects.

In support of these studies, we also carried out a high resolution study of the microwave spectrum of calcium Rydberg states. The results are described in a thesis,[7] and in the publications listed below.

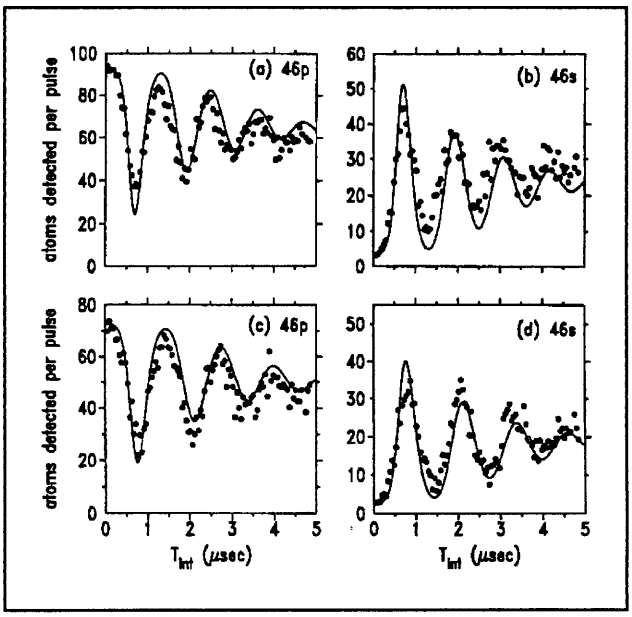

Figure 4. Comparison of calculated and observed evolution of the system for large ensembles of atoms in the cavity. The filled circles are the number of atoms detected in the 46p and 46s states as a function of atom-cavity interaction time T_{int}. The amplitudes of the theory curves are scaled to compare with data but there are no other adjustable parameters. (a) and (b): $\bar{N} = 380$. (c) and (d): $\bar{N} = 300$.

Publications

Gentile, T.R., B.J. Hughey, T.W. Ducas, and D. Kleppner. "Experimental Study of Two-Photon Rabi Oscillations." Paper presented at the Sixth Conference on Coherence & Quantum Optics, Rochester, New York, June 1989.

Gentile, T.R. *Microwave Spectroscopy and Atom-Photon Interactions in Rydberg States of Calcium.* Ph.D. diss. Dept. of Physics, MIT, 1989.

Gentile, T.R., B.J. Hughey, T.W. Ducas, and D. Kleppner. "Microwave Spectroscopy of Calcium Rydberg States." *Phys. Rev. A.* Accepted for publication.

Hughey, B.J., T.R. Gentile, T.W. Ducas, and D. Kleppner. "A Split High Q Superconducting Cavity." Submitted to *Rev. Sci. Instrum.*

[7] T.R. Gentile, *Microwave Spectroscopy and Atom-Photon Interactions in Rydberg States of Calcium,* Ph.D. diss. Dept. of Physics, MIT, 1989.

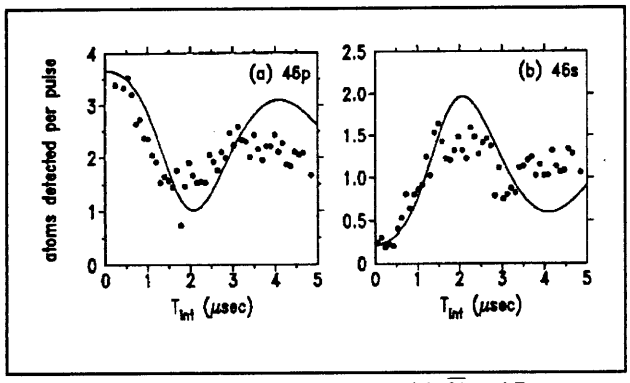

Figure 5. Similar to figure 4, but with $\bar{N} = 15$.

Hughey, B.J., T.R. Gentile, T.W. Ducas, and D. Kleppner. "Experimental Study of Small Ensembles of Atoms in a Microwave Cavity." Submitted to *Phys. Rev. A.*

Hughey, B.J., T.R. Gentile, T.W. Ducas, and D. Kleppner. "Atom-Photon Interaction Modified by a Microwave Cavity." Paper presented at the Sixth Conference on Coherence & Quantum Optics, Rochester, New York, June 1989.

Hughey, B.J, T.R. Gentile, D. Kleppner, and T.W. Ducas. "A Study of One- and Two-Photon Rabi Oscillations." *Phys. Rev. A.* 40:5103 (1989).

Hughey, B.J. *Cavity Modified Atom-Photon Interaction.* Ph.D. diss. Dept. of Physics, MIT, 1989.

2.2 Rydberg Atoms in a Magnetic Field

Sponsor

National Science Foundation
Grant PHY 87-06560

Project Staff

George R. Welch, Chun-Ho Iu, Long Hsu, Michael W. Courtney, Professor Daniel Kleppner

A hydrogen atom in a strong magnetic field poses a fundamental challenge to atomic theory. The Hamiltonian looks almost trivial, but, in fact, no general solution yet exists and important aspects of the problem remain a mystery. If the atom is in a low-lying energy state, the magnetic effect can be

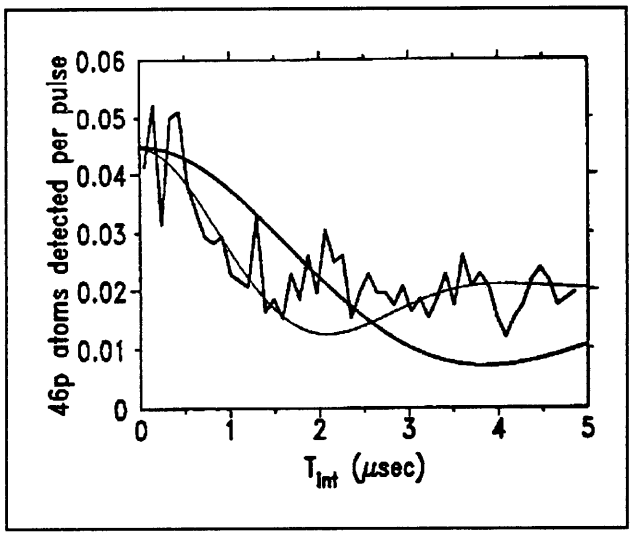

Figure 6. Observation of the time evolution with a single atom in the cavity. The solid curves are calculations for $Q = 1.5 \times 10^6$, T = 1.95K (dark line) and T = 9K (light line).

treated as a perturbation. However, for an atom in a Rydberg state, the magnetic interaction is comparable to the Coulomb interaction and perturbation theory fails completely. Although calculations based on diagonalizing as many as 200,000 basis states were carried out, theorists cannot yet predict energy levels for high-lying Rydberg states and for positive energy (continuum) states. Experiments are essential for guiding new theoretical approaches.

Our research centers on high resolution spectroscopy of Rydberg atoms in a magnetic field. Recent results include the study of: (1) anticrossings between energy levels, which provide information on mixing between levels in a regime of "approximate symmetry"; (2) quantum behavior in the regime where the classical system exhibits strong chaotic motion; and (3) energy level structure and ionization mechanisms when the energy is above the ionization limit.

The experiment employs two c.w. dye lasers to excite an atomic beam of lithium inside of a superconducting solenoid. (Lithium is essentially hydrogen-like, but with small differences which are of some interest in their own right.) The first laser excites the atom from the 2S to the 3S state by a two-photon transition; the second laser excites the atom to a Rydberg state with a single photon. Atoms which are excited to Rydberg states

are detected by electric field ionization in a region outside of the excitation region. The wavelength of the second laser is measured by using an etalon as a transfer standard between the Rydberg lines and iodine absorption lines. (The iodine lines and the free spectral range of the etalon are themselves calibrated relative to the zero-magnetic field lithium Rydberg spectrum.) The resolution and absolute energy accuracy are $\sim 10^{-3}cm^{-1}$. The magnetic field is determined by exciting $|\Delta m| = 1$ transitions and measuring the paramagnetic splitting of the n=21 manifold.[8] The accuracy in field is $\sim 10^{-4}T$.

"Level repulsion," the tendency for energy levels to avoid crossing each other as the magnetic field is changed, provides information on the coupling between levels. We studied level repulsion effects due to the presence of lithium core electrons. In addition, we studied the level repulsion that occurs due to the inherent nature of the diamagnetic interaction. Figure 7 shows the first experimental study of level repulsion due to the diamagnetic interaction. The disappearance of the *lower* state is a characteristic feature which distinguishes this anticrossing from a lithium core-induced anticrossing. The diamagnetic anticrossing is a result of a breakdown of an approximate symmetry of the system. The theory for this anticrossing, which is close to the region of complete chaos, is still not complete.[9]

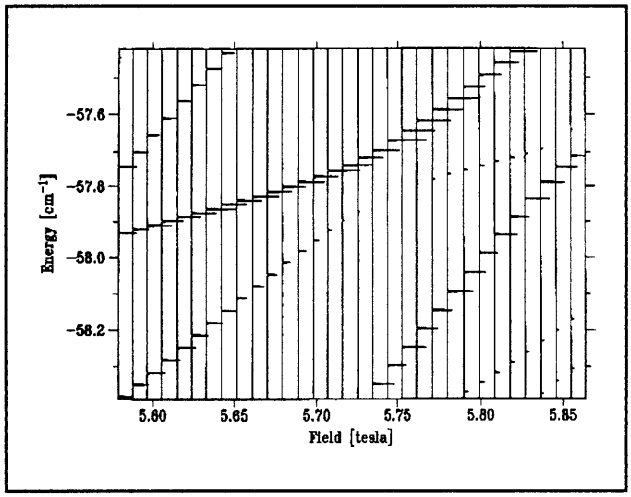

Figure 7. An example of a diamagnetic anticrossing induced by the breakdown of an approximate symmetry.

When the energy is above the zero point energy of the free electron-magnetic field system, the atom can spontaneously ionize. We observed the first high resolution spectra near and above the ionization limit.[10] Figure 8 shows some of these spectra. We discovered many narrow resonances in this regime. The lifetimes of the narrow resonances are greater than a few thousand cyclotron periods. Such long lifetimes are unexpected on the basis of classical studies.

We also found that states which approach the ionization limit form a series similar to the Rydberg series of the unperturbed atoms. Moreover, we discovered additional Rydberg-like series that each converge to one of a sequence of Landau levels. The system behaves as if the motion were separable. Because the atom-magnetic field system is confined in the direction perpendicular to the magnetic field, the quantum states extend along the magnetic field direction and behave like a one-dimensional hydrogen atom. As a result, traverse Landau energy is simply added to the longitudinal Rydberg energy. The discovery of orderly structure in a regime that is believed to be chaotic suggests that either the connection between quantum mechanics and chaos is not well understood, or that a good deal of order is possible in a region of chaos. Systematic study is continuing on the structure and linewidth of the positive energy resonances and the mechanisms of ionization.

During this past year, we have also carried out the first high resolution study of the atom-magnetic field system in the regime where classical motion undergoes a transition from regular to chaotic motion. The com-

---

[8] M.M. Kash, G.R. Welch, C. Iu, and D. Kleppner, *Spectrochemica Acta A* 45: 57 (1989).

[9] D. Delande and J.C. Gay, *Phys. Rev. Lett.* 57: 2006 (1986).

[10] G.R. Welch, M.M. Kash, C. Iu, L. Hsu, and D. Kleppner, *Phys. Rev. Lett.* 62: 1975 (1989); C. Iu, G.R. Welch, M.M. Kash, L. Hsu, and D. Kleppner, *Phys. Rev. Lett.* 63: 1133 (1989).

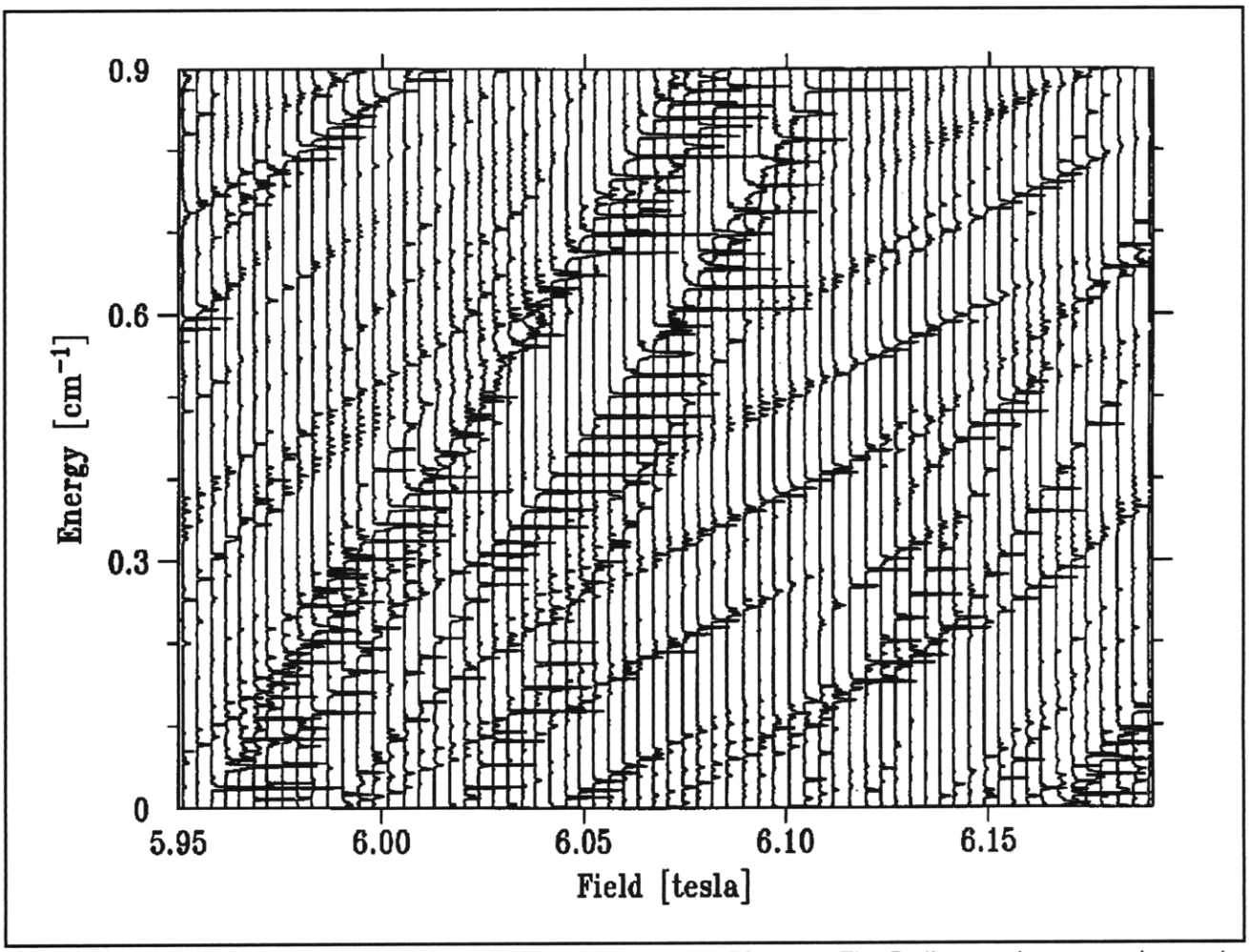

Figure 8. Positive energy spectra with magnetic field increments 50 gauss. The Rydberg series converging to the second Landau level can be seen as parallel and equal spaced levels with a slope of 1.7cm^{-1}/T.

monly used tool for the study of quantum chaos is energy level statistics. Such studies require locating and resolving each level in a pure sequence, for example odd parity, m=0 states. The task becomes experimentally difficult when the system approaches chaos because small electric fields can cause mixing with states of opposite parity, and a small misalignment of the polarization can introduce states of $m = \pm 1$. Consequently, theoretical guidance is required to identify the states in the particular sequence under study. Figure 9 shows our recent progress in calculating levels for high Rydberg states in a magnetic field. The calculation is done by diagonalizing about 2,700 states of lithium using an IBM RT computer.

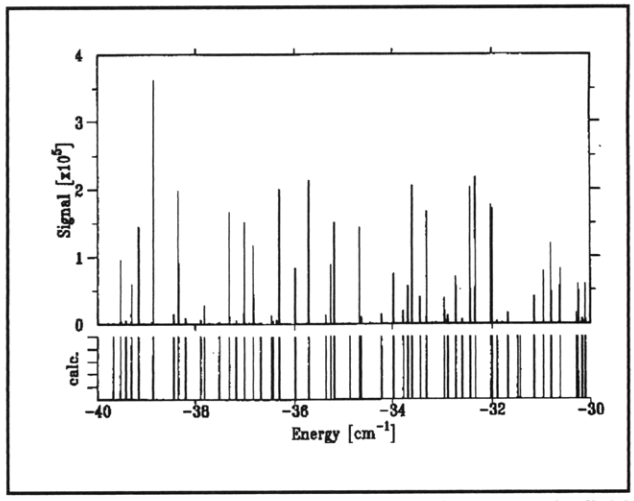

Figure 9. Spectrum of lithium atom in magnetic field of 6.1 T. Above: Experimental spectrum. Below: Calculated spectrum. The difference between experiment and calculation is less than 10^{-2}cm^{-1}.

Publications

Iu, C-H., G.R. Welch, M.M. Kash, L. Hsu, and D. Kleppner. "Orderly Structure in the Positive Energy Spectrum of a Diamagnetic Rydberg Atom." *Phys. Rev. Lett.* 63: 1133 (1989).

Kash, M.M., G.R. Welch, C-H. Iu, and D. Kleppner. "Diamagnetic Structure of Lithium n≈21," *Spectrochemica Acta* 45A: 57 (1989).

Welch, G.R., M.M. Kash, M. Michael., C-H. Iu, L. Hsu, and D. Kleppner. "Positive Energy Structure of the Rydberg Diamagnetic Spectrum." *Phys. Rev. Lett.* 62: 1975 (1989).

Welch, G.R., M.M. Kash, C-H. Iu, L. Hsu, and D. Kleppner. "Experimental Study of Energy Level Statistics in a Regime of Regular Classical Motion." *Phys. Rev. Lett.* 62: 893 (1989).

Welch, G.R. *High Resolution Spectroscopy of Rydberg Atoms in a Magnetic Field.* Ph.D. diss. Dept. of Physics, MIT, 1989.

2.3 Millimeter-Wave Measurement of the Rydberg Constant

Sponsor

National Science Foundation
Grant PHY 87-06560

Project Staff

Pin P. Chang, Scott Paine, Robert P. Lutwak, James P. Schwonek, Professor Daniel Kleppner

The Rydberg constant R is prominent among the fundamental constants as the primary atomic standard of length. Recent experiments determined R to an accuracy of nearly one part in 10^{10}, using optical spectroscopy.[11] The limitation to these measurements is not the inherent precision of the experiment but the accuracy of the wavelength standard. It is now generally accepted that optical wavelengths cannot be compared to a precision greater than 1 part in 10^{10}. One consequence of this limitation is that length is now defined in terms of the distance traveled by light in a fixed time interval, rather than in terms of a certain number of optical wavelengths. Thus, wavelength measurements of R appear to have reached a natural barrier.

We are attempting to advance the precision of R by measuring it in frequency units. (The specific quantity we shall measure is cR). We shall accomplish this by measuring millimeter wave transitions between Rydberg states of hydrogen. Because the frequency of millimeter radiation can be measured to the full precision of modern atomic clocks, the experiment is not limited by metrological standards.

The goal of our experiment is three-fold: First is the reevaluation of R itself. Second is the measurement of the Lamb shift. Because our measurements involve high angular momentum states for which the Lamb shift is extremely small, a comparison of our results with optical measurements can yield an improved value of the Lamb shift. Third is the precise frequency calibration of the spectrum of hydrogen to allow an independent check of optical frequency metrology as it starts to advance.

We are determining the Rydberg constant by measuring the frequency of the $|n = 29 \rightarrow n = 30|$ "circular" transition in atomic hydrogen, using the Ramsey separated oscillatory field method. The experiment is designed to achieve an accuracy of 1 part in 10^{11}, an order of magnitude improvement over the present state of the art.[11] The transition frequency, 256 GHz, is low enough to allow us to use established techniques to phase lock our millimeter-wave source directly to a cesium primary frequency standard.

At the time of our last progress report, we had completed construction of an atomic

[11] F. Biraben et al., *Phys. Rev. Lett.* 62: 621 (1989); Zhao et al., *Phys. Rev. Lett.* 58: 1293 (1987); M.G. Boshier et al., *Nature* 330: 463 (1971).

beam apparatus with a cold (10K–80K) atomic hydrogen source and had demonstrated the population of the n=29 state by two-photon absorption via the 2p state, and the adiabatic transfer of the atoms to the high angular momentum state via the crossed fields method of Delande and Gay.[12]

During the past year, we experimented with an alternative excitation scheme for the Rydberg state, using three-step excitation to n=29 through the 2p and 3s states. This effort included the development of a single-mode tunable pulsed YAG-pumped titanium sapphire laser. For the present, however, we have returned to our original method. Also, we developed a flexible, CAMAC-MAC-based data acquisition system. Using this, we studied the hydrogen intensity and dissociation within the discharge (see figure 10). The system is also being applied to numerous tasks in the diagnosis and control of the apparatus.

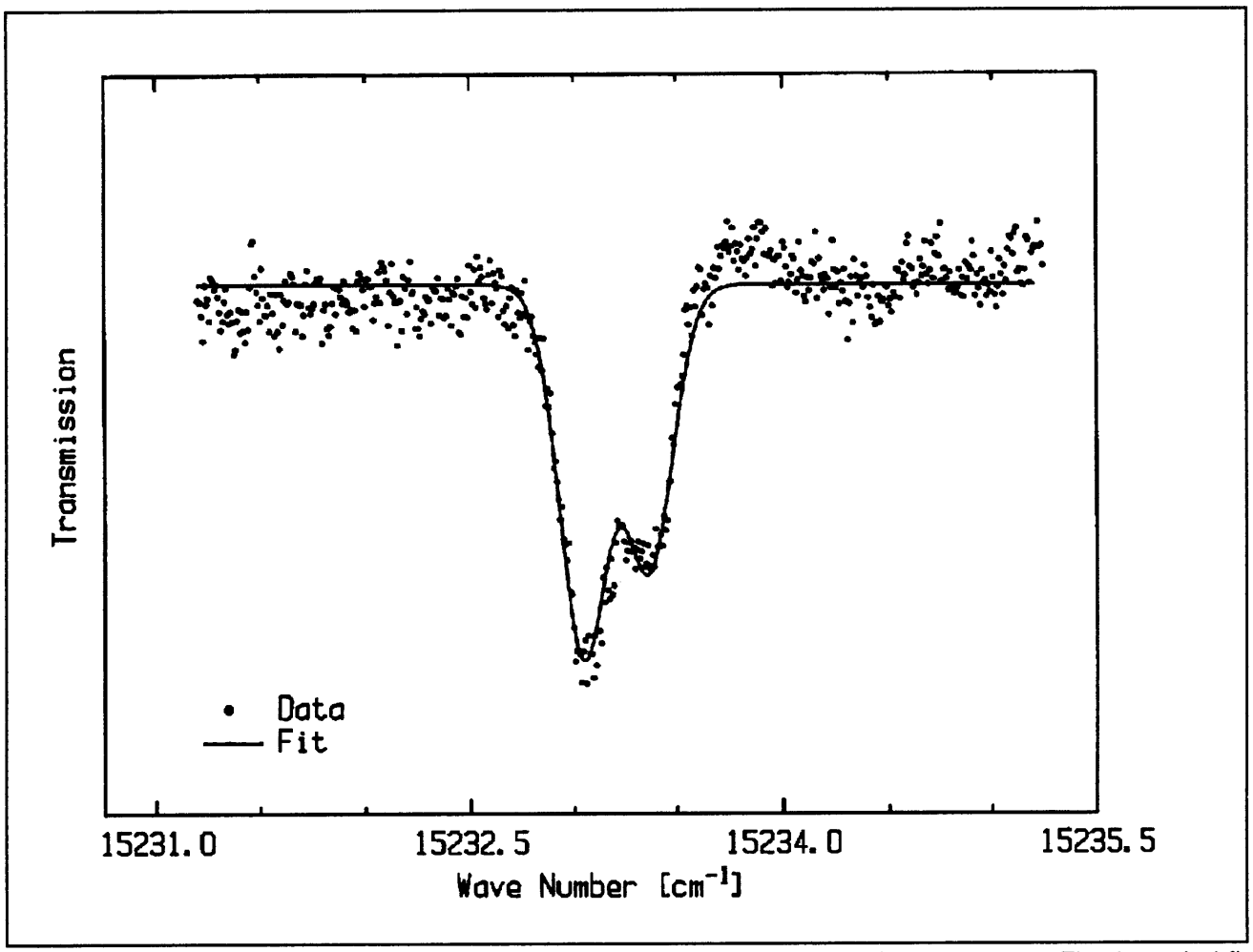

Figure 10. Transmission of pulsed dye laser through the rf discharge in the atomic beam source. The theoretical fit to the doppler-broadened spectrum indicates a discharge temperature of approximately 400 K. The hydrogen is subsequently cooled to produce a 10-80 K atomic beam.

The millimeter wave system is a critical element in the experiment. We have continued the development of quasi-optical components for the manipulation and detection of the millimeter wave radiation, including lenses, beamsplitters, and

[12] D. Delande and J. C. Gay, *Europhys. Lett.* 5:303 (1988).

polarizers. A scanned antenna-coupled pyroelectric detector system has been developed for mapping the millimeter wave beam profiles. A map of the radiation profile at the atomic beam is shown in figure 11.

We have begun designing the controlled field region in which the actual measurement will take place and hope to complete construction of the apparatus in the coming year. Efforts are also continuing to optimize the hydrogen beam source and the efficiency of the circular state production.

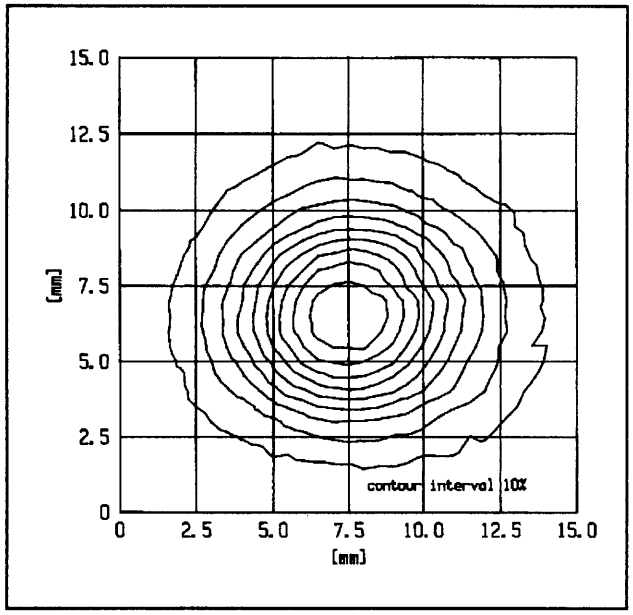

Figure 11. Intensity profile of the 256 GHz radiation used to drive the n = 29 → n = 30 circular transition.

2.4 Precision Mass Spectroscopy of Ions

Sponsors

Joint Services Electronics Program
Contract DAAL03-89-C-0001
National Science Foundation
Contract PHY 86-05893

Project Staff

Kevin R. Boyce, Eric A. Cornell, Deborah Kuchnir, Professor David E. Pritchard

In 1989, we made the first mass comparison of single trapped ions, raising the state of the art for fractional precision in mass measurement to 4×10^{-10}. This is a first step toward our ultimate goal of determining the mass of individual atomic and molecular ions with precisions of 10^{-11} or better. This precision will give us the capability of making experiments that address issues in both fundamental and applied physics:

- The $^3H^+ - {}^3He^+$ mass difference is important in ongoing experiments to measure the electron neutrino rest mass.
- Excitation and binding energies of typical atomic and molecular ions can be determined by weighing the small decrease in energy: $\Delta m = E_{bind}/c^2$.
- Experiments that weigh γ-rays can be used in a new method to determine Avogadro's number, N_A, a key fundamental constant whose accurate determination would permit the replacement of the artifact mass standard by an atomic mass standard.
- Traditional applications of mass spectroscopy should benefit from the several orders of magnitude improvement in both accuracy and sensitivity which our approach offers over conventional techniques.

In our experimental approach, we measure ion cyclotron resonance on a single molecular or atomic ion in a Penning trap, a highly uniform magnetic field with axial confinement provided by weaker electric fields. We monitor ions, oscillating along magnetic field lines, by the currents induced in the trap electrodes. Working with only a single ion is essential because space charge from other ions leads to undesired frequency shifts. This work in trapping and precision resonance draws on techniques developed by Hans Dehmelt at the University of Washington and Norman Ramsey at Harvard University, for which they shared the 1989 Nobel Prize.

Our most notable accomplishment this year was determining the carbon monoxide-molecular nitrogen mass ratio to an accuracy

of 4×10^{-10}.[13] The ratio of the cyclotron frequencies of the two ions is the inverse of the ratio of the masses as long as the magnetic field remains constant. By trapping first a single N_2^+ ion and measuring its frequency, and then swapping to a single CO^+ ion, and then back again to N_2^+, we are able to correct for drifts in the magnetic field to about 0.5 parts per billion (see figure 12).

We have developed techniques for driving, cooling, and measuring the frequencies of all three normal modes of Penning trap motion. Thus, we can manipulate the ion position reproducibly to within 30 microns of the center of the trap, correcting for electrostatic shifts in the cyclotron frequency to great accuracy. We use a π-pulse method to coherently swap the phase and action of the cyclotron with the axial modes.[14] Therefore, although we detect only the axial motion directly, we can determine cyclotron frequency by measuring how much phase accumulates in the cyclotron motion in a known time interval (see figure 13).

Currently, precision is limited by magnetic field imperfections and temporal instabilities. Achieving our long range goal of 10^{-11} precision requires either dramatic improvements in field stability or simultaneous comparison of two different ions. With two ions of equal charge, the ion-ion perturbations are very similar for each ion and, hence, do not introduce significant uncertainty in the mass ratio. Our group has succeeded in trapping a single CO^+ ion and a single N_2^+ ion simultaneously.[15] In the coming year, we plan to develop techniques for making precision resonance measurements on two ions simultaneously.

Publications

Cornell, E.A., R.M. Weisskoff, K.R. Boyce, R.W. Flanagan, G.P. Lafyatis, and D.E. Pritchard. "Single-Ion Cyclotron Resonance Measurements of $M(CO^+)/M(N_2^+)$." *Phys. Rev. Lett.* 63:1674 (1989).

Cornell, E.A., R.M. Weisskoff, K.R. Boyce, and D.E. Pritchard. "Mode Coupling in a Penning Trap: π Pulses and a Classical Avoided Crossing." *Phys. Rev. A* 41:312 (1990).

Kuchnir, D.L. *Trapping and Detecting Two Different Single Ions at Once: A Step Towards Ultra-High-Precision Mass Comparison Measurements.* B.S. thesis. Dept. of Physics, MIT, 1989.

2.4.1 Atom Interferometry

Sponsors

Joint Services Electronics Program
Contract DAAL03-89-C-0001
U.S. Army Research Office
Contract DAAL03-89-K-0082
U.S. Navy - Office of Naval Research
Contract N00014-89-J-1207

Project Staff

Chris R. Ekstrom, David W. Keith, Bruce G. Oldaker, Quentin Turchette, Professor David E. Pritchard

Using fabricated transmission gratings as optical elements for the matter waves, we are constructing an atom interferometer to physically separate atom waves before recombining them. This interferometer will be useful in studies of atomic properties, tests of basic quantum physics, for metrology, as rotation sensors, and, perhaps, ultimately as devices to make ultra-small structures using atom holograms.

---

[13] E.A. Cornell, R.M. Weisskoff et al., *Phys. Rev. Lett.* 63:1674 (1989).

[14] E.A. Cornell, R.M. Weisskoff et al., *Phys. Rev. A* 41:312 (1990).

[15] D.L. Kuchnir, *Trapping and Detecting Two Different Single Ions at Once: A Step Towards Ultra-High-Precision Mass Comparison Measurements,* B.S. thesis, Dept. of Physics, MIT, 1989.

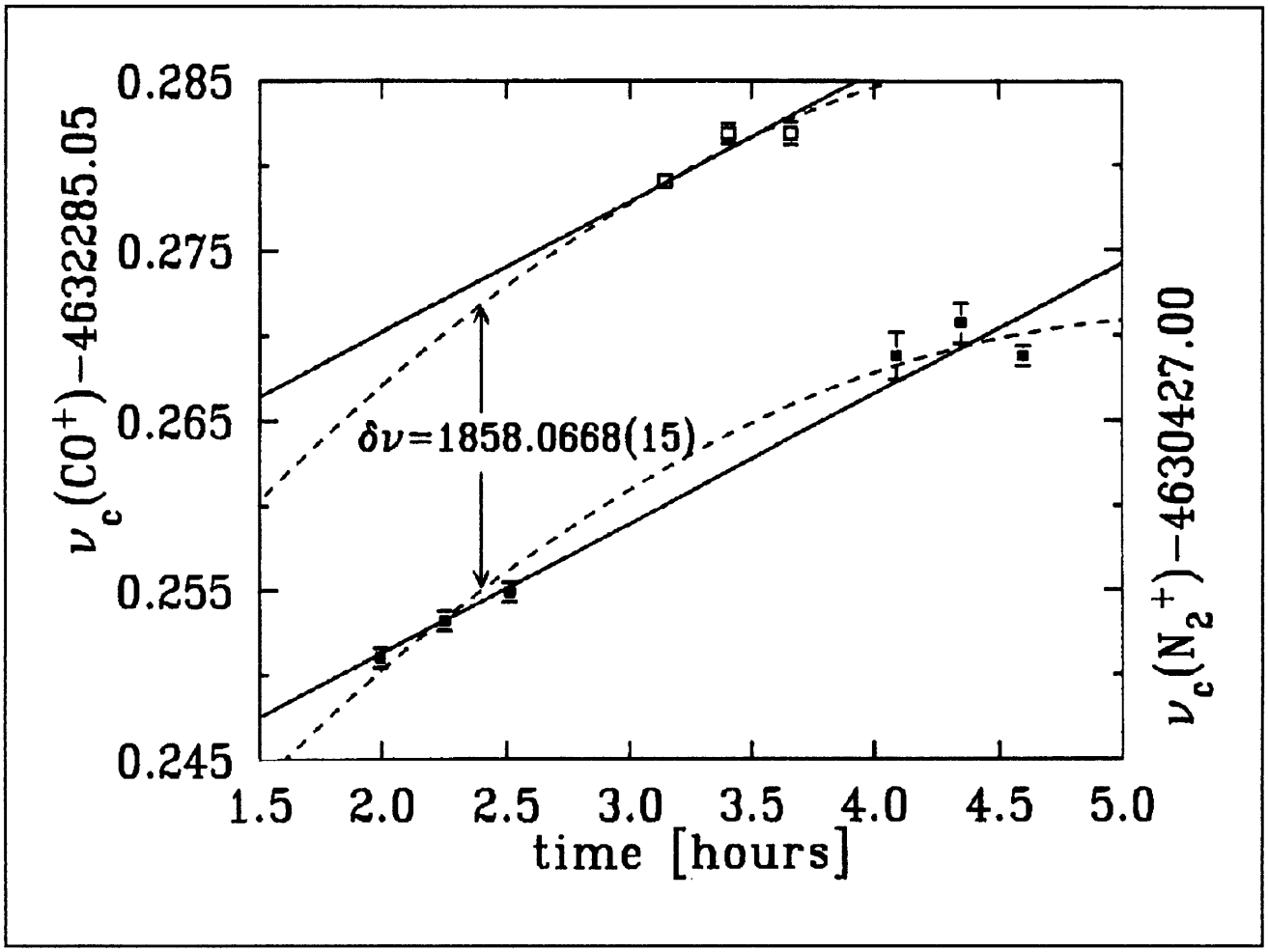

Figure 12. The data from a mass comparison run are shown. The solid squares (open squares) are the cyclotron frequency of $N_2^+(CO^+)$. A total of three ions were loaded in the order $N_2^+ - CO^+ - N_2^+$. The solid lines are a fit to the two frequencies assuming a field drift that is linear in time. The dotted-line assumes a quadratic field drift. The indicated value for the difference frequency results from the latter assumption, and corresponds to $M(CO^+)/M(N_2^+) = 0.9995988876(3)$.

During the last year, our atom interferometer evolved from a rough plan to an essentially complete device. At present, we have tested all its major components at least once. We will test the complete system during the coming year.

Our interferometer consists of three 0.2 μm-period diffraction gratings equally spaced $\sim$ 0.65 m apart in our atomic beam machine. The maximum separation of the beams will be $\sim 60\mu$m. The first two gratings separate and redirect the atomic beam forming a standing wave interference pattern in the atomic flux at the third grating, which acts like a mask to sample this pattern.

We can estimate our anticipated final signal strength from the properties of the individual gratings. Attenuation caused by the primary grating and the grating support structure gives an intensity in the 0^{th} order of $\sim$ one-eighth of the incident intensity and one-sixteenth in each of the $\pm$ 1 orders. The final intensity detected at the maximum of a fringe after transmission through all three gratings can be calculated by summing the amplitudes for the two sides of the interferometer and will be 0.005 of the incident intensity. The fringe constant will be 4 to 1, so the interference signal will be 0.004 of the incident intensity. We are anticipating that the final interference signal through the interferometer will be $\sim 4 \times 10^3$ counts per second. This should generously exceed the noise of the detector (≤ 100 sec^{-1}).

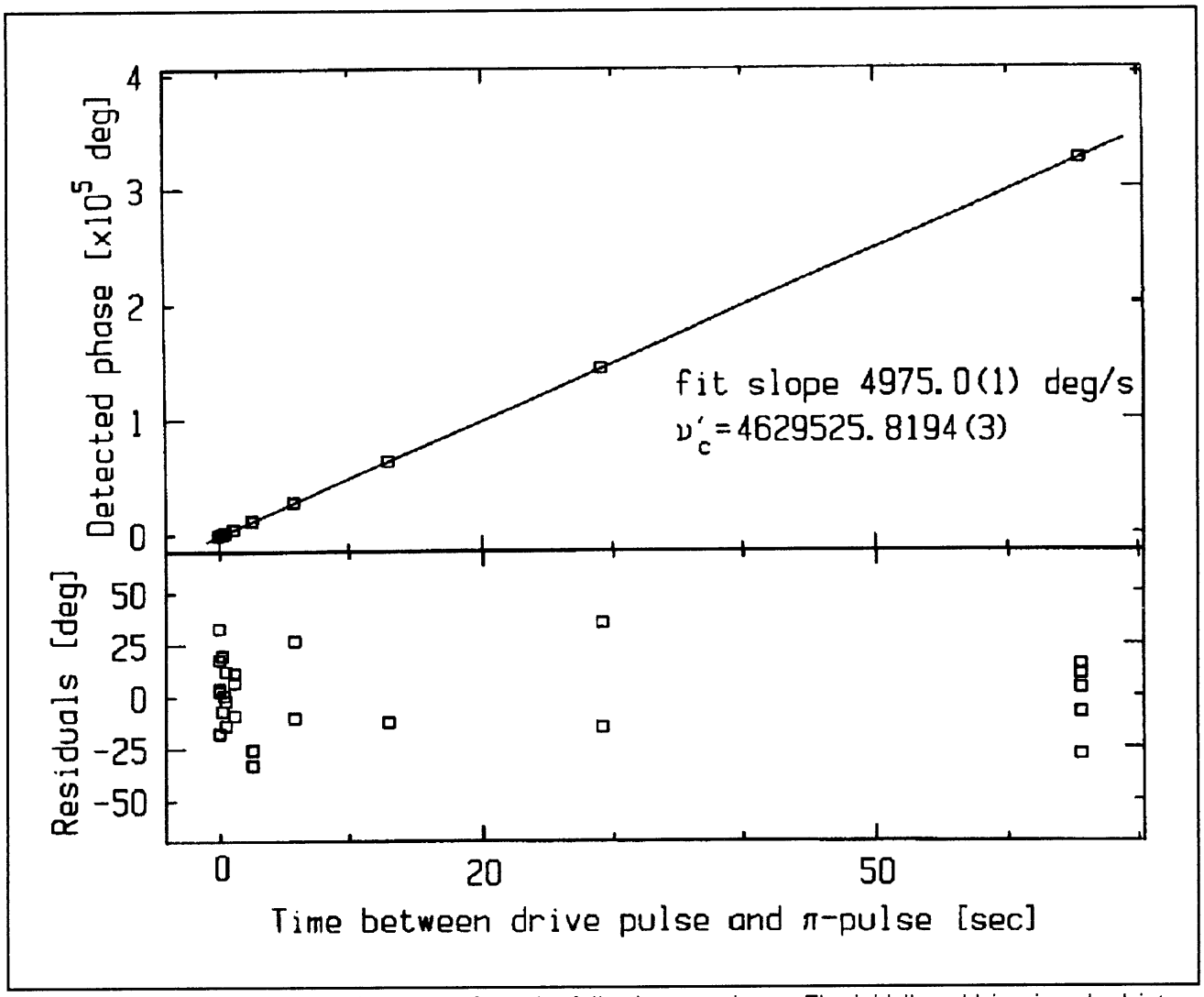

Figure 13. For each plotted point, we perform the following experiment: The initially cold ion is pulsed into a cyclotron orbit of known initial phase and then allowed to evolve "in the dark" for an indicated amount of time, t. Then a pulse is applied which exchanges cyclotron and axial motions, bringing the ion's cyclotron action and phase into the axial mode. As the ion's axial motion rings down, its phase is detected. The appropriate multiple of 360° is added, and a line is fitted to the points. The slope of the line is the frequency difference between the frequency generator and the trap cyclotron frequency.

The mechanical vibrations of our machine are a principal technical obstacle because they could blur the interference pattern. There are two types of required limits on vibrations. First, the three gratings must move relative to each other by less than $\sim 1/4$ period (50 nm) during the time the final grating samples the intensity at a given position. Thus, the rms amplitude of relative vibrations integrated over all frequencies greater than the reciprocal of the integration time must be less than $\sim$ 50 nm. The second requirement is related to the motion of the gratings due to acceleration of, or rotation about, the center of mass of the grating system during the 1.3 ms time it takes for the atoms to traverse the interferometer. This means that below $\sim$ 900 Hz the rms acceleration must be less than $10^{-2}ms^{-2}$, and the rms angular velocity must be less than 10^{-5} radians per second.

We have solved our vibration problem by using a combination of passive isolation and active feedback. The passive isolation system consists of small pneumatic feet which act like damped springs to support the machine and give it a 3-Hz resonant frequency. This isolates the machine from building noise at higher frequencies. We have used the active feedback system to stabilize the relative posi-

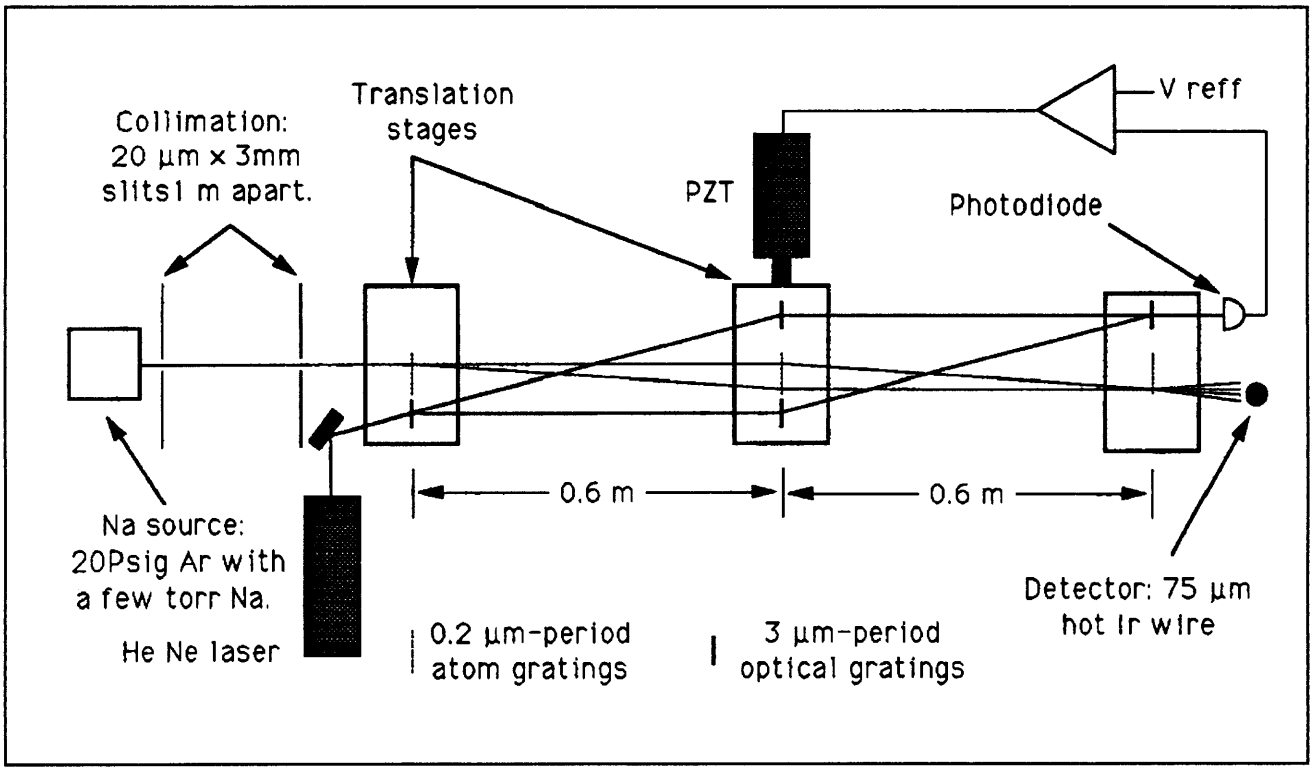

Figure 14. Our current atom interferometer with laser interferometer vibration isolation system is shown. (Not to scale.)

tions of the three gratings at frequencies below ~ 150 Hz. This system works best at low frequencies < 10 Hz) where the passive system is least effective. The reduction of relative motion provided by the active system will allow us to use much longer integration times when we are looking for the interference signal. The active feedback system uses a laser interferometer which has the same transmission grating geometry as the atom interferometer. We mounted the gratings for the optical interferometer on the same three translation stages as the matter wave gratings to record the exact relative orientation of the matter wave interferometer. We apply the signal from the optical interferometer to provide a measure of the relative alignment of the three grating platforms to a Piezoelectric translator (PZT) through a feedback network to stabilize the platforms (figure 14). With this system, we have adequately reduced the relative rms motion (at frequencies less than 0.3 Hz) of the gratings from ~ 1500 to 40 nm. We also reduced the rms acceleration in a frequency range to which the interferometer is sensitive from 1.1×10^{-2} to $2.3 \times 10^{-3} ms^{-2}$, which is safe by a factor ~ 5, ensuring sufficiently low angular velocities of the apparatus.

We have also made significant progress in overcoming another technical obstacle, the relative alignment of the atom gratings. For all points along the height (3 mm) of our ribbon shaped beam to have the same phase of interference signal, the gratings must be aligned to an angle of $\sim 10^{-5}$ rads. with respect to rotations about the beam axis. We accomplished this by using a technique based on the optical polarizing properties of the gratings.

In addition to the work on vibrations and alignment mentioned above, our main progress during 1989 was construction of the various mechanical components that position the gratings inside the vacuum envelope. Also, we have written computer software and built electronic hardware to control the position of the three grating platforms and the detector, and the height, angle and position of the second collimating slit. Instead of directly varying the voltage of the PZT that controls the position of the last grating, now we will use the computer to vary the null point of the active feedback

system when we are searching for interference fringes.

When we have successfully demonstrated this interferometer, our first experimental objective will be a demonstration of Berry's phase with bosons. Another experiment could be an improved measurement of the Aharonov-Casher effect.

Publications

Keith, D.W., and D.E. Pritchard. "Atom Optics." In *New Frontiers in QED and Quantumoptics.* New York: Plenum Press. Forthcoming.

Keith, D.W., M.L. Schattenburg, H.I. Smith, and D.E. Pritchard. "Diffraction Gratings from Atoms." *QELS Conference,* Baltimore, Maryland, April 1989.

Oldaker, B.G., P.J. Martin, P.L. Gould, M. Xiao, and D.E. Pritchard. "Experimental Study of Sub-Poissonian Statistics in the Transfer of Momentum from Light to Atoms." Submitted to *Phys. Rev. Lett.*

Pritchard, D.E., and B.G. Oldaker. "Light Forces and Atom Diffraction: An Illustrated Summary." Paper presented at the *Sixth Conference on Coherence,* Rochester, New York, 1989.

Pritchard, D.E. Experimental Studies of Atom Diffraction and the Mechanical Forces of Light on Atoms, *NICOLS Conference.* Bretton Woods, New Hampshire: Academic Press, 1989.

2.5 Neutral Atom Trap

Sponsors

U.S. Navy - Office of Naval Research
Contracts N00014-83-K-0695 and N00014-89-J-1207

Project Staff

Kristian Helmerson, Michael A. Joffe, Dr. Min Xiao, Ke-Xun Sun, Professor David E. Pritchard

We have trapped large numbers of neutral atoms, and cooled them to millikelvin temperatures. Our next objective is to cool them to microkelvin temperatures. Dense samples of atoms cooled to microkelvin temperatures promise to open up new and exciting areas of physics. The lack of interaction of the low velocity atoms due to their reduced thermal motion, together with the possibility of indefinitely long interaction times, make samples of trapped atoms ideal for high resolution spectroscopy and for use as atomic frequency standards. High density samples of ultra-cold atoms will also make possible new studies of interatomic collisions and collective effects, such as Bose condensation. We have made progress using our existing magnetic trap. In addition, we started a new project to develop a continuous source of slow atoms to load into future magnetic traps.

2.5.1 Magnetic Trap for Neutral Atoms

Now that techniques for trapping neutral atoms are well established,[16] the field of neutral atom trapping has moved from infancy to adolescence and the emphasis is now on doing experiments with the trapped atoms.

Currently, our main effort in neutral atom trapping is cooling trapped atoms to low temperatures. While this remains a difficult and elusive goal (to date, we have only achieved microkelvin temperatures with untrapped atoms), the rewards for supercooling trapped atoms are significant. The long confinement times, together with the reduced thermal motion of cold atoms, could result in a new era of ultra-high resolution spectroscopy and precise frequency standards. Potentially more exciting is the possibility of combining the high densities achievable in traps and the long deBroglie

[16] D.E. Pritchard, K. Helmerson, and A.G. Martin, "Atom Traps," in *Atomic Physics,*. 11, eds. S. Haroche, J.C. Gay, and G. Grynberg (Singapore: World Scientific, 1989), pp. 179-97.

wavelength of ultra-cold atoms to observe novel quantum collective phenomena.

At present, we are trying to demonstrate cyclic cooling of magnetically trapped neutral atoms.[17] A combined laser and radio frequency cooling scheme should allow us to cool our atoms to microkelvin temperatures. During the past year, we tried a newly designed cyclic cooling scheme that operates in a magnetic field of less than 300 gauss. (We currently trap atoms at a minimum field of 1500 gauss.) We have modified our superconducting magnets so that our trap operates at low magnetic fields. This modification, resulting in improved decoupling of the trapped atoms from the powerful slowing laser, could allow us to load more atoms into the trap than was previously possible. In addition, we have made many other modifications to the magnetic trap to optimize detection of cooled atoms and to extend the lifetime of the trapped atoms. We plan to test this trap during 1990.

As the only group in the world capable of doing both rf and laser spectroscopy of trapped atoms, we have performed laser fluorescence and absorption spectroscopy of magnetically trapped sodium atoms. Currently, we are analyzing the data from this research. Studying the theory of the radiative decay of densely confined atoms, we have found a substantial modification of the spontaneous decay rate of trapped atoms due to their quantum statistics. Finally, we completed a study of the Zeeman-tuned laser slowing process in the magnetic trap.[18]

2.5.2 Slow Atom Source

During 1989, we began building a simple, intensive and continuous source of slow atoms which can also separate the atoms from the laser light used to slow them. Separating the atoms is a crucial requirement, permitting additional low intensity laser light to collimate, focus and cool the slow beam further. This source of slow atoms is useful for loading traps or for atomic beam experiments because we do not have to introduce intense slowing laser light.

The technique we developed uses a continuous "zeeman slower,"[19] a spatially varying magnetic field, to compensate the changing Doppler shift of the atoms in the slowing process and a second orthogonal laser beam to deflect and extract the slowed atoms. This simple, compact system has a 25-cm long zeeman slower and ignores atoms which start with thermal velocities greater than 600 meters/second. Since it slows only the low velocity portion of the Maxwell-Boltzman distribution, a low oven temperature (about 180 centigrade) is desirable. With this low temperature, the slower needs a large orifice to provide the requisite flux.

The major difficulty in making a continuous and intense slow atomic beam is in effectively extracting slowed atoms from the strong, slowing laser beam. We will extract the slowed atoms in a region of low magnetic field by using light pressure from a beam with two frequencies to circumvent optical pumping to hyperfine levels not excited by the laser. Figure 15 shows the configuration of the experimental arrangement.

In the zeeman slower, the slowing laser slows atoms with velocities smaller than 600 meters/second at position a to about 150 meters/second at position b where the magnetic field is held near zero. The deflection

---

[17] D.E. Pritchard, "Cooling Neutral Atoms in a Magnetic Trap for Precision Spectroscopy," *Phys. Rev. Lett.* 51:1336-39 (1983).

[18] V.S. Bagnato, G.P. Lafyatis, A. Martin, K. Helmerson, J. Landry, and D.E. Pritchard, "Laser Deceleration and Velocity Bunching of a Neutral Sodium Beam," *J. Opt. Soc. Am. B* 6: 2171-77 (1989).

[19] J.V. Prodan, W.D. Phillips, and H. Metcalf, *Phys. Rev. Lett.* 49:1148 (1982).

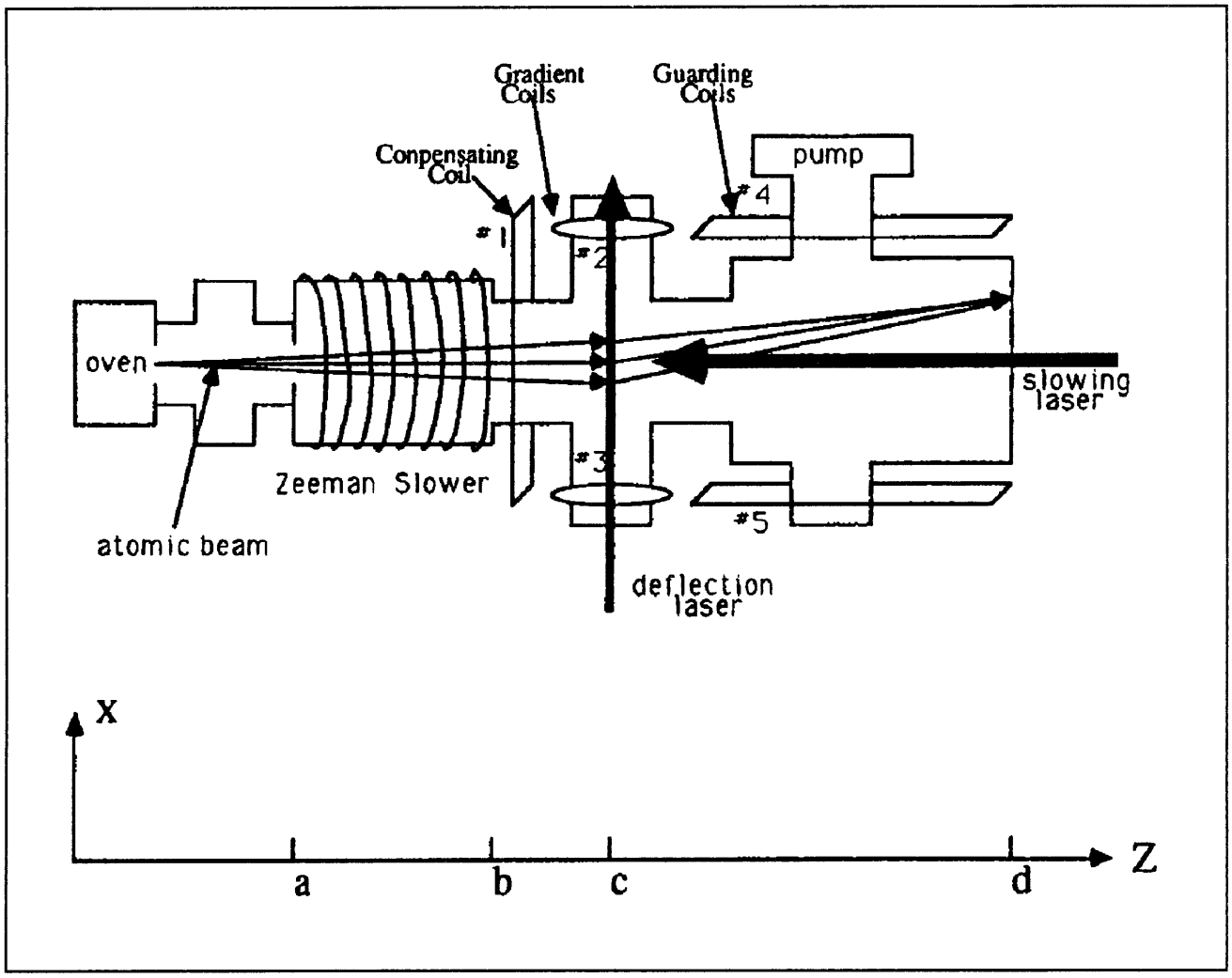

Figure 15. Schematic diagram of the slow-atom source.

laser deflects atoms slowed further by the intense slowing laser beam to velocities below 100 meters/second at c. c is right circular polarized with a strong sideband spaced at 1.77 GHz to repump the F=1 ground state atoms. So far, we have observed slowing of nearly 10^{10} atoms per second with photodetectors mounted inside the zeeman slower.

Publications

Bagnato, V.S., G.P. Lafyatis, A. Martin, K. Helmerson, J. Landry, and D.E. Pritchard. "Laser Deceleration and Velocity Bunching of a Neutral Sodium Beam." *J. Opt. Soc. Am. B*: 2171 (1989).

Gallagher, A., and D.E. Pritchard. "Exoergic Collisions of Cold Na*-Na." *Phys Rev. Lett.* 63:957 (1989).

Gould, P.L., P.J. Martin, G.A. Ruff, R.E. Stoner, J-L. Picque, and D.E. Pritchard. "Momentum Transfer to Atoms By a Standing Light Wave; Transition From Diffraction to Diffusion." Submitted to *Phys. Rev. Lett.*

Pritchard, D.E. "Atom Optics." In *McGraw-Hill Yearbook of Science and Technology.* Forthcoming.

Pritchard, D.E., K. Helmerson, and A.G. Martin. "Atom Traps." In *Proceedings of the 11th International Conference on Atomic Physics.* Paris, 1988.

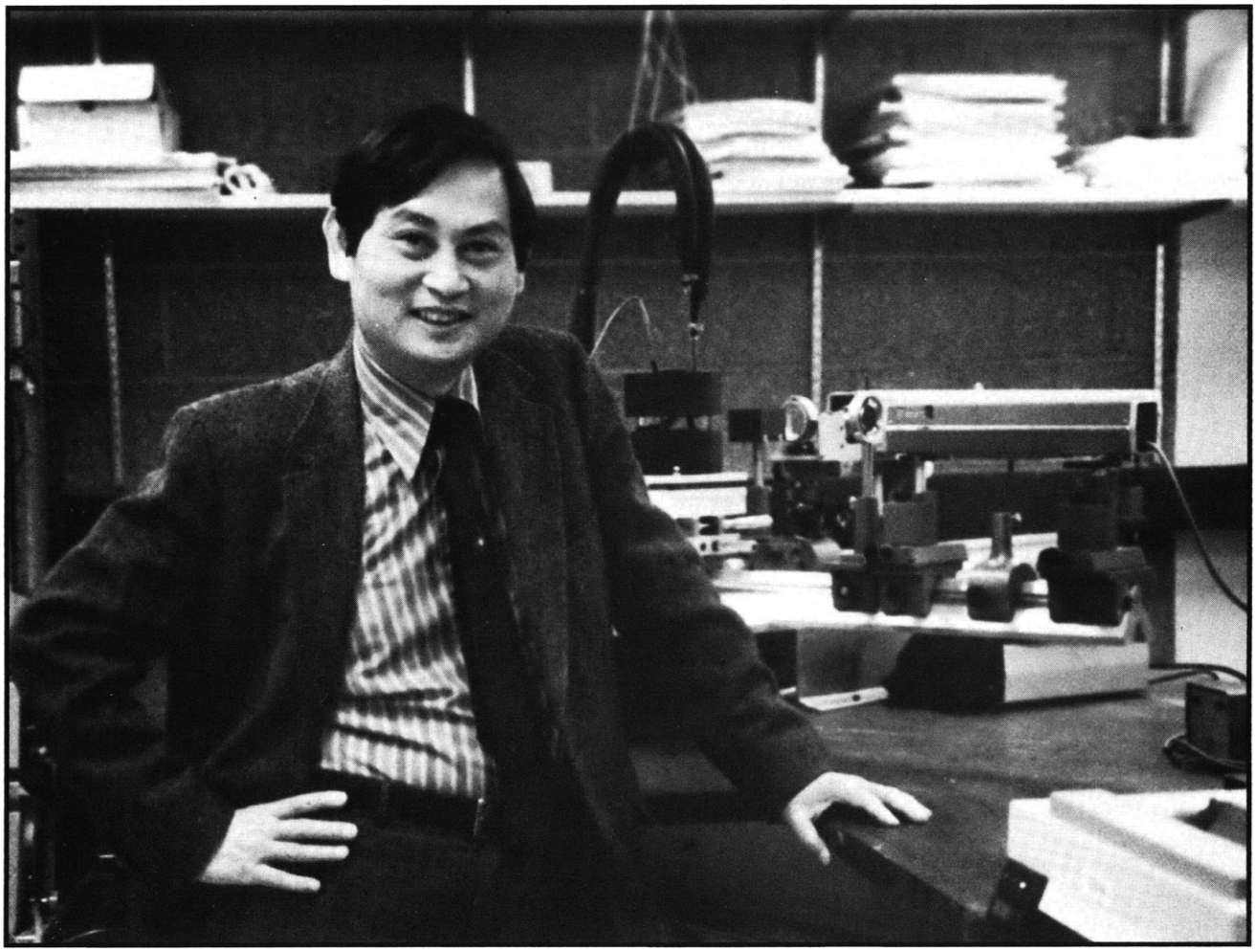

Professor Sow-Hsin Chen